Design and experiment of the variable rate fertilization system for soybean and maize strip compound planting

Li Ding, Kaixuan Wang, Yechao Yuan, Yuanyuan Li, Huanhuan Chen, Zheng Zhang, Qianyi Wang, Changchang Yu, He Li*

(*College of Mechanical & Electrical Engineering, Henan Agricultural University, Zhengzhou 450002, China*)

Abstract: In view of the existing composite planting cannot do independent control of fertilizer rate for each row, and fertilizer is easy to moisture solidification caking and rely on a single way to measure the speed of inaccurate problems, a split-drive variable fertilizer application system was designed for soybean and maize strip cropping composites. It includes roller crushing bi-directional spiral fertilizer discharger, split-drive variable fertilizer application system and 'GNSS + encoder' dual speed measurement system. By modeling agglomerated fertilizer particles, discrete element simulation was carried out to analyze the crushing effect. The speed measurement error variation folds of both GNSS and encoder under different speed conditions were obtained through field speed measurement tests. Finally, 4.5 km/h was identified as the switching point between the two speed measurements. Through bench testing, a mathematical relationship model was developed for the soybean and maize belts in terms of 'Fertilizer Application Rate - Operating Travel Speed - Metering Mechanism Rotor Speed', and the results are presented in the table below. Fertilizer discharge consistency was verified for fertilizer dischargers. Field trials were conducted, and the results show: The soybean belt had a maximum error of 4.81% at a fertilizer application rate of 150 kg/hm^2 and an operating speed of 5 km/h; the maximum error in the corn belt was 4.67% at a fertilizer application rate of 600 kg/hm^2 and operating speed of 4 km/h. Both have a maximum error of less than 5%, which meets the requirements for variable fertilizer application.

Keywords: variable fertilization, EDEM simulation, soybean corn compound planting, spiral fertilizer apparatus

DOI: 10.25165/j.ijabe.20251806.9691

Citation: Ding L, Wang K X, Yuan Y C, Li Y Y, Chen H H, Zhang Z, et al. Design and experiment of the variable rate fertilization system for soybean and maize strip compound planting. Int J Agric & Biol Eng, 2025; 18(6): 122–134.

1 Introduction

Reasonable variable fertilization is an important factor to ensure the yield of soybean and corn compound planting. The common planting mode of soybean and maize strip composite planting in Huang-Huai-Hai region is '4:2' planting mode. At present, the fertilizer application machine generally adopts the outer groove wheel fertilizer discharger, which has the problems of low fertilizer discharge, pulsation of fertilizer discharge, unevenness, fertilizer agglomeration and blockage. Moreover, it is impossible to exactly and independently regulate the amount of fertilizer discharged from soybean and corn, and it is difficult to realize the differential precision fertilization of soybean and corn belts under the strip compound planting mode.

The fertilizer discharger is the core working part of variable rate fertilization. At present, scholars have carried out a lot of research on the performance improvement of fertilizer distributors. Xu et al.[1] designed a centrifugal cavity disc extrusion type fertilizer discharger for the problem of large amount of fertilizer and easy to jam in the direct seeding of rape high-speed machine, and the fertilizer discharge process was smooth and stable. Xiao et al.[2] designed four-head spiral double rows of fertilizer discharger for oilseed rape direct seeding machine to achieve double rows in one machine, which reduces the phenomenon of fertilizer discharge pulse. Wang et al.[3] designed a conical disc push-plate double-row fertilizer discharger to improve the stability and uniformity of the paddy field side deep fertilization and fertilizer discharger, and the double-row fertilizer discharge amount was consistent. In order to improve soil fertility and fertilizer utilization rate, Qi et al.[4] designed a deep loosening variable speed fertilizer applicator, which had good deep loosening performance and variable fertilization index. In order to improve the fertilizer use efficiency of direct sowing and transplanting rice, Kemoh Bangura et al.[5] designed a six-line deep fertilizer applicator with good fertilization accuracy. In terms of variable rate fertilization, Campbell et al.[6] designed a double disc fertilizer spreader, which controls the opening of the hydraulic flow proportional valve and the speed of the turntable, and combines the forward speed of the machine to perform variable rate fertilization. The Flexi-Coil series of variable rate fertilizer planters developed by Case Company in the United States can be

Received date: 2025-01-15 **Accepted date:** 2025-09-10

Biographies: Li Ding, PhD, Associate Professor, research interest: agricultural equipment and control system, Email: dingli@henau.edu.cn; **Kaixuan Wang**, MS candidate, research interest: agricultural equipment and control system, Email: 1244994189@qq.com; **Yechao Yuan**, MS candidate, research interest: agricultural equipment and control system, Email: yuanyechao@stu.henau.edu.cn; **Yuanyuan Li**, MS candidate, research interest: agricultural equipment and control system, Email: lyy18749019024@163.com; **Huanhuan Chen**, MS candidate, research interest: agricultural equipment and control system, Email: 2026839066@qq.com; **Zheng Zhang**, MS candidate, research interest: agricultural equipment and control system, Email: 1060949081@qq.com; **Qianyi Wang**, MS candidate, research interest: agricultural equipment and control system, Email: 1789185971@qq.com; **Changchang Yu**, PhD, Lecturer, research interest: agricultural equipment and control system, Email: yuchang@henau.edu.cn.

***Corresponding author: He Li**, PhD, Professor, research interest: design and control of agricultural equipment. College of Mechanical and Electrical Engineering, Henan Agricultural University, Zhengzhou 450002, China. Tel: +86-18310047256, Email: chungbuk@163.com.

adjusted for different types of fertilizers and seeds[7]. In order to improve the accuracy and uniformity of fertilization, Shi et al.[8] designed a centrifugal variable rate fertilizer applicator with good fertilization efficiency. Chang et al.[9] developed control software with integration of multi-sensor information to achieve the granular fertilizer spreader variable release control. The above research focuses on the structural optimization and variable control of the net fertilizer discharger, and does not pay attention to the crushing of agglomerated fertilizer particles and the differential split-drive precision fertilization of soybean and corn required by the agronomic requirements of the composite planting mode. In this paper, aiming at the problems that the existing compound planting cannot control the amount of fertilizer discharged by each fertilizer discharging monomer independently, the fertilizer is easy to be wet and solidified, and the variable rate fertilization relies on a single method to measure the speed inaccuracy, a soybean-maize strip compound planting sub-drive variable rate fertilization system was designed, including a two-way spiral fertilizer discharger for roller crushing, a sub-drive variable rate fertilization system, and a 'GNSS + encoder' double speed measurement system. The performance of variable rate fertilization was verified by field experiments.

2 Roll crushing bidirectional screw fertilizer discharger design

2.1 Structural design of fertilizer discharger

The overall structure of the roller crushing two-way spiral fertilizer discharger is shown in Figure 1. The fertilizer discharger is mainly composed of roller crushing device, two-way spiral fertilizer discharge shaft, transmission system, and other components.

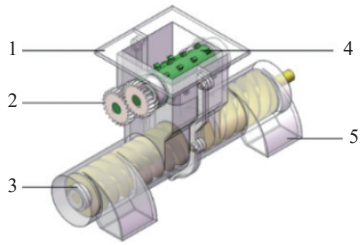

1.Shell 2.Transmission system 3.Bidirectional spiral fertilizer shaft 4.Roll crushing device 5.Fertilizer outlet

Figure 1 Structure diagram of two-way spiral fertilizer discharger with roller crushing

According to the 375 kg/hm^2 fertilization amount stipulated in the 'GB/T35487-2017 variable rate fertilization seeder control system', that is, 375 kg/hm^2, the parameters of the two-way spiral fertilizer discharge shaft were determined. Considering the increase of pitch and the decrease of fertilizer filling rate[10], combined with the spatial structure of the test seeder, the final structural parameters of the designed bidirectional spiral fertilizer discharge shaft are as follows: The internal diameter of the screw d_1=20 mm, the external diameter D_1=60 mm, the pitch P_1=40 mm, the depth of the screw h=20 mm, and the average thickness of the screw b=2 mm. According to Equation (1)[11], the theoretical maximum speed of the two-way spiral fertilizer shaft is n_{max}= 204.12 r/min.

$$n_{max} \le \frac{C}{\sqrt{D_1}} \tag{1}$$

where, n_{max} is the critical speed of the fertilizer spiral, r/min; D_1 is fertilizer spiral outer diameter, 60 mm; C is material comprehensive coefficient, referring to the 'transport machinery design selection manual' value C=50.

When the two-way spiral fertilizer discharger is used for fertilizer discharge, the fertilizer particles in the fertilizer box enter the fertilizer discharger under the action of gravity. The stepping motor drives the two-way spiral fertilizer discharge shaft to rotate, promotes the fertilizer particles to move along the spiral axis, and transports them to the fertilizer discharge ports on both sides. Finally, the fertilizer particles are discharged from the fertilizer discharger under the action of gravity, falling into the fertilizer discharge pipe until the soil, and the fertilizer discharge process is completed. According to the working principle of the screw conveying mechanism[12], the relationship between the amount of fertilizer discharged by the single row of the two-way spiral fertilizer shaft can be calculated according to Equations (2) and (3):

$$q = [\pi(D_1^2 - d_1^2)P_1/4 - bhL_p]\rho\varphi \tag{2}$$

$$Q = qn_1t \tag{3}$$

where, q is single-turn fertilizer discharge amount of a single fertilizer outlet of a bidirectional spiral fertilizer discharger, g; the average length of L_p is screw, mm; ρ is fertilizer particle density, ρ_{urea}=0.001 236 g/mm^3; $\rho_{diammonium\ phosphate}$=0.001 635 g/mm^3; φ is filling coefficient, here taken as 0.33[13]; Q is total amount of fertilizer, g; t is time, min; n_1 is rotating speed of fertilizer apparatus, r/min.

By substituting the fertilizer density ρ of urea and diammonium phosphate into Equation (2) respectively, the theoretical fertilizer discharge amount of the single row fertilizer mouth of the spiral fertilizer discharger can be obtained: when the fertilizer discharger is applied with corn fertilizer, the single-turn fertilizer discharge amount is q_{corn}= 38.8 g, and when the soybean fertilizer is applied, the single-turn fertilizer discharge amount is $q_{Soybean}$= 51.4 g.

The power required for the fertilizer discharge of the fertilizer discharge device is calculated according to the calculation Equation (4) in the international standard 'ISO 7119-1981 loose material continuous handling equipment screw conveyor drive power design rule' to calculate the power required for the screw fertilizer discharge device to transport the fertilizer particles:

$$P_2 = \frac{Q_1(\lambda L_1 \pm H_1)}{367} + \frac{D_1L_1}{20} \tag{4}$$

where, P_2 is power required for fertilizer discharge, kW; Q_1 is fertilizer delivery, t/h; l_1 is fertilizer horizontal projection distance, 0.32 m; λ is running resistance coefficient, with reference to the national standard 'JB/T7679-2008 screw conveyor' value of 1.1; h_1 is fertilizer vertical projection height, and this paper uses spiral auger horizontal placement, so it is 0 m.

Take the density of the largest diammonium phosphate fertilizer to calculate the required power, two-way spiral fertilizer discharger two rows of fertilizer single circle discharged fertilizer amount of 102.8 g, take the highest speed n_{max} 204.12 r/min, Q_1= 1.258 t/h, and then get P_2= 21.6 W. Required stepping motor power in accordance with Equation (5)[14]:

$$P_3 = \xi\frac{P_2}{\eta} \tag{5}$$

where, P_3 is required drive motor power, W; ξ is power reserve coefficient, generally 1.2-1.4, here taken as 1.3; η is motor transmission efficiency, here η=0.9. After calculation, the required drive motor power P_3=31.2 W was obtained.

Fertilizer discharger rotational speed η_1 is adjusted by the microcontroller through obtaining the speed of machine operation and combining it with the amount of fertilizer applied per hm^2 S.

The theoretical relationship between the operating speed v_0 of the integrated machine for soybean and corn banded composite planting and sowing and fertilizer application and the rotational speed of the fertilizer discharger η_1 is deduced as in Equation (6):

$$n_1 = \frac{S \times 15 \times 1000 \times 60 l_1}{666.7q} \cdot v_0 \tag{6}$$

where, S is fertilizer set for soybean or corn, kg/hm^2; q_{corn}=38.8 g, $q_{Soybean}$= 51.4 g; l_1 is soybean-maize strip compound planting sowing and fertilization machine operation width, l_1=1.25 m; v_0 is fertilization operation speed, m/s.

2.2 Roll crushing device design

Aiming at the problems that urea granular fertilizer is easy to be wet and agglomerated, resulting in uneven fertilization and poor operation quality, a roller crushing device is designed to crush the agglomerated particles in fertilizer.

2.2.1 Structure design of roller crushing device

The roller crushing device consists of two differential rollers. The circumference of each roller is evenly distributed to crush the roller teeth of the caking fertilizer particles, and its shape and size directly affect the crushing effect of the caking fertilizer. Referring to the relevant research of Chen et al.[15] of China Agricultural University, the design reference equations of roll mass m_1, roll diameter d_2, and roll length l_2 (7) are as below:

$$\begin{cases} d_2 = \dfrac{q_n \phi}{\chi \sin^2 \beta_0} \\ m_1 = \dfrac{\pi d_2^2 - \pi (d_2 - 2R_i)^2}{4} \rho_1 l_2 \end{cases} \tag{7}$$

where, d_2 is roll diameter, mm; ρ_1 is material density of roller, ρ_1=1240 kg/m^3; q_n is crushing ratio, value 0.4; ϕ is the diameter of the fertilizer block after crushing, taking the target value of 20 mm; x is minimum diameter correction factor, taking 0.8; the friction angle between β_0 is caking fertilizer particles and roller teeth is 30°; r_i is roll wall thickness, mm. Through Equation (7), the diameter of the roller d_2=40 mm and the length of the roller l_2=100 mm are determined.

Referring to the design principle of roller crusher, the external dimension of roller teeth of roller crushing device should be smaller than the size of lumpy fertilizer particles. At the same time, in order to improve the fertilizer discharging capacity, the shape of fertilizer crushing roller teeth is designed based on the mining prismatic conical tooth shape[16], as shown in Figure 2. In order to ensure the strength of the fertilizer crushing roller teeth and increase the ability of the fertilizer crushing roller teeth to bite the fertilizer lumps, the angle of inclination of the top of the teeth θ is 80°[17].

Under the condition that the diameter of the roller d_2=40 mm and the center distance of the two crushing rollers A_1=50 mm, in order to ensure the crushing effect, the height of the roller teeth should not exceed the particle size of the crushed fertilizer particles, so the height H_2 of the roller teeth should meet Equations (8) and (9). The tooth width b_1 and the tooth thickness b_2 are designed according to the strength of the crushed material, and calculated according to Equation (10)[18]:

$$\frac{A - d_2}{2} \le H_2 \le A - d_2 \tag{8}$$

$$H_2 = 0.6(A - d_2) \tag{9}$$

$$\begin{cases} b_1 = 0.7 H_2 \\ b_2 = 0.8 H_2 \end{cases} \tag{10}$$

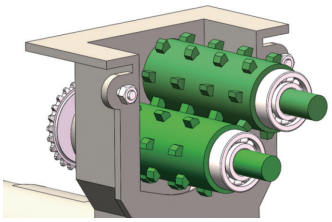

a. Three-dimensional schematic diagram of roller crushing device

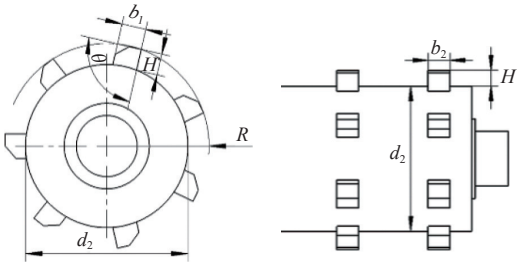

b. Tooth profile parameter diagram

Figure 2 Schematic diagram of roller crushing device

Together with the above equations, when the center distance is determined to be 50 mm, the two pairs of roller teeth have a certain overlap in the axial direction. In theory, the crushing effect of the fertilizer block is improved, with the roller tooth height H_2=6 mm, tooth width b_1=4.2 mm, and tooth thickness b_2=4.8 mm. The more the number of toothed rollers with uniform distribution on the circumference of the roller, the smaller the space of the adjacent roller teeth will be, which will reduce the crushing effect on large-sized agglomerated fertilizer[15]. According to Equation (11)[19], the number of roller teeth in the circumferential direction of a single roller is:

$$N_1 = \frac{2\pi(R_1 - H_2)}{d_3} \tag{11}$$

where, R_1 is roll radius, 20 mm; d_3 is the distance between two adjacent teeth in the cross section of the roller, mm.

Bidirectional spiral fertilizer discharge device pitch P_1=40 mm; because it is a double-ended spiral, two spiral surface spacing of 20 mm. Therefore, the caked fertilizer particles need to be less than 20 mm in diameter after crushing, then need to be d_3<20 mm, to find the N_1>4.398. Here the value of N_1 is 7.

2.2.2 Calculation of crushing capacity

The cross-section diagram of the roller crushing device is shown in Figure 3. The reference equation for the productivity of the roller crushing device per unit time (12)[20] is:

$$Q_2 = 1 \times 10^{-9} \rho k (V_1 - V_2) \tag{12}$$

where, ρ is fertilizer particle density, kg/m^3; k is filling coefficient; V_1 is fertilizer volume per unit time through the roller device, mm^3/h; V_2 is the volume of the roll device turned per unit time, mm^3/h.

$$V_1 = 30 n_2 \pi l_2 (2A_1^2 + d_4^2 - 4R_1^2 - 2A_1 d_4) \tag{13}$$

$$V_2 = 60 n_2 N_1 V_3 \tag{14}$$

where, n_2 is roller rotation speed, r/min; d_4 is roller radius after adding the height of roller teeth, mm; V_3 is volume of individual roll teeth, mm^3.

Substituting Equations (13) and (14) into Equation (12), Equation (15) is obtained, which is the productivity of the roller crushing device.

$$Q_2 = 3\times10^{-3}\rho K n_2\left[\pi l_2(2A_1^2+d_4^2-4R_1^2-2A_1d_4)-2N_1V_3\right] \quad (15)$$

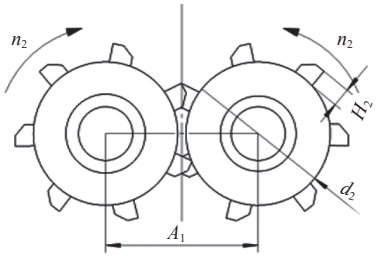

Figure 3 Cross section of roller crushing device

2.2.3 Useful power calculation

The useful power refers to the energy consumed by the roller crushing device to crush the fertilizer particles in unit time, which is an important parameter of the roller crusher. The useful power of the roller crushing device is calculated using Equation (16)[21]:

$$P_4 = Q_2 W \quad (16)$$

where, Q_2 is roll crushing device productivity, t/h; W is energy required for breaking unit fertilizer, kW·h/t.

The calculation of the energy required for crushing unit fertilizer by the roller device is shown in Equation (17):

$$W = 11W_i\left(\frac{1}{d_5^j}-\frac{1}{d_6^j}\right) \quad (17)$$

where, W_i is bond work index; d_5 is particle size of fertilizer after crushing; d_6 is particle size of fertilizer before crushing; j is the calculating index, generally set as 0.2-1.4.

Substituting Equation (17) into Equation (16), the useful power of the roller crushing device is:

$$P_4 = 11Q_2W_i\left(\frac{1}{d_5^j}-\frac{1}{d_6^j}\right) \quad (18)$$

Because the roller crushing device only plays a role in crushing the agglomerated fertilizer particles, the loose fertilizer particles slide directly from the gap between the shell of the fertilizer discharger and the crushing device, which does not affect its normal application. Therefore, the theoretical productivity Q_2 of the roller crushing device obtained by V_1 and V_2 is greater than the actual required productivity, and the derived useful power P_4 of the roller crushing device is also greater than the actual required power. Because the particle size d_6 of the fertilizer before crushing changes greatly, and the particle size d_5 of the fertilizer after crushing is inconsistent, it is inaccurate to use the theoretical power calculation equation to calculate the required power of the equipment under actual production conditions[22]. In this paper, the actual particle crushing test was carried out by selecting different types of stepper motors to drive the roller crushing device, and the stepper motor of BYGH1186A4J was finally selected.

3 Discrete element simulation of roller crushing device

EDEM is a CAE software that uses discrete element method to simulate granular materials. It can simulate loose materials such as coal mines and stones[23-25]. EDEM can also be coupled with other CAE software, RecurDyn, Fluent, etc., to help engineers quickly design and analyze, and speed up the progress of the task. Considering that the amount of urea fertilizer required by the corn belt is large, and the urea is susceptible to moisture caking, this paper only conducts EDEM discrete element simulation on the crushing process of the caking urea fertilizer.

3.1 Simulation parameters and model construction

The relevant literature[26] was consulted to obtain various properties of urea as listed in Table 1.

Table 1 EDEM parameter settings of urea granules

Item	Attribute	Numerical value
Urea grains	Poisson ratio	0.25
	Elastic modulus/Pa	8.5×10^7
	Density/kg·m^{-3}	1236
Fertilizing shaft, shell	Poisson ratio	0.394
	Density/kg·m^{-3}	1240
Urea-urea	Coefficient of restitution	0.11
	Coefficient of static friction	0.3
	Coefficient of rolling friction	0.1
Urea-fertilizer shaft, shell	Coefficient of restitution	0.41
	Coefficient of static friction	0.32
	Coefficient of rolling friction	0.18

The size of urea fertilizer particles after caking was measured, and the caking fertilizer model was established by using SolidWorks software with reference to the relevant size. The model was imported into EDEM software and filled with urea particles. Each particle was adhered by the bonding model in EDEM to establish the BPM model of urea fertilizer block. As a part of the caking fertilizer, each small urea particle that constitutes the caking fertilizer particle can independently calculate the parameters in the crushing process through its Poisson's ratio, elastic modulus, density, and other parameters, and obtain a more realistic calculation value. By consulting the relevant literature, the Hertz-Mindlin with bonding model is used to bond small particles into large materials. When the most normal force and tangential force are reached, the bonding bond breaks, so as to achieve the crushing and fracture effect of granular materials. The normal stiffness coefficient and tangential stiffness coefficient between the crushing simulation particles of the agglomerated fertilizer in this paper are obtained by Equations (19) and (20).

$$k_n = \frac{4}{3}\left(\frac{1-v_1^2}{E_1}+\frac{1-v_1^2}{E_2}\right)^{-1}\cdot\left(\frac{r_1+r_2}{r_1\cdot r_2}\right)^{-\frac{1}{2}} \quad (19)$$

$$k_s = \left(\frac{1}{2}\sim\frac{2}{3}\right)k_n \quad (20)$$

where, k_n, k_s are normal and tangential stiffness coefficients of particles, N/m^3; E_1, E_2 are modulus of elasticity of particle 1, particle 2, Pa; r_1, r_2 are particle 1, radius of particle 2, mm; v_1 is Poisson's ratio of urea particles, 0.25.

After calculation, the relevant data shown in Table 2 are obtained.

Table 2 Urea fertilizer particle adhesion parameter tab

Name	Parameter	Numerical value
Urea grains	Unit normal stiffness/N·m^{-3}	1.0×10^6
	Unit tangential stiffness/N·m^{-3}	5.0×10^6
	Critical normal stress/Pa	4.0×10^4
	Critical tangential stress/Pa	2.5×10^4
	Bonding radius/mm	2.5

The API program of Hertz-Mindlin with bonding model is used to construct the adhesion model of agglomerated fertilizer particles by filling small urea particles, as shown in Figure 4.

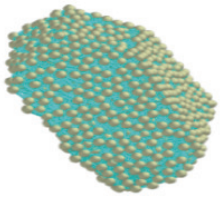

Figure 4 BPM module of the fertilizer block after the bonding key is generated

3.2 Crushing simulation and analysis

According to the data in Table 1 and Table 2, the material properties, particle properties, caking fertilizer model and particle generation parameters in the particle factory required for EDEM simulation are set up. The simulation time was set to 4 s with a time step of 0.001 s. The first 1s was used to generate the particles, and the large particles were replaced with the agglomerated fertilizer BPM model constructed above at 0.4 s, as shown in Figure 5.

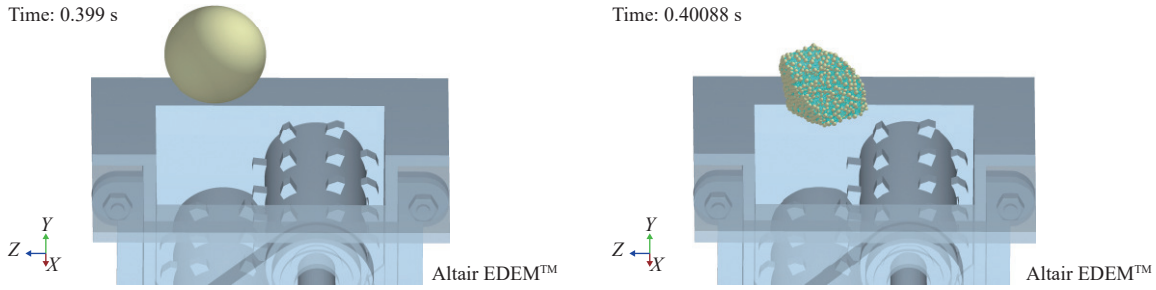

a. 0.399 s caked particles before replacement b. 0.400 s after the replacement of agglomerated particles

Figure 5 EDEM particle replacement process

Since the roller crushing device does not affect the normal application of loose fertilizer particles, this paper sets the roller speed to a fixed 300 r/min[15], and the simulation process is shown in Figure 6.

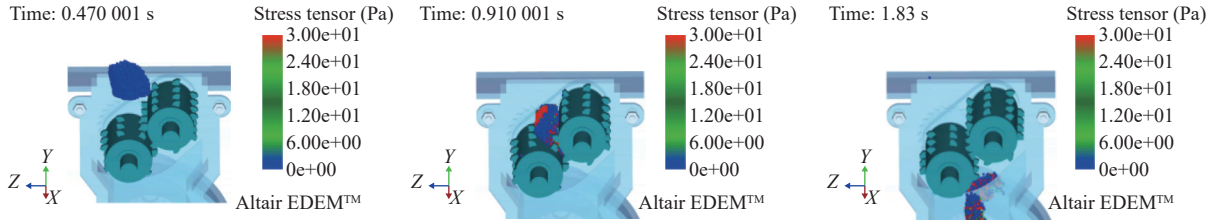

a. Fertilizer particles before crushing b. Fertilizer granules in crushing c. After crushing of fertilizer particles

Figure 6 EDEM simulation process of caking fertilizer particle crushing

After the crushing simulation is completed, the change of the bonding key in the crushing process of the caking fertilizer is derived through the data analysis and post-processing function of the EDEM software, and the line chart shown in Figure 7 is obtained. From Figure 7, it can be seen that when the simulation is carried out to 0.4 s, due to the use of the BPM model of caking fertilizer to replace the large particles, the number of bonding keys suddenly increases. As the caking fertilizer falls into the roller crushing device, the bonding keys are gradually destroyed until the end of the simulation. The failure rate reaches 74.6%, and the broken fertilizer fragments are smaller than the pitch of the fertilizer discharger, as shown in Figure 8, which proves that the roller crushing device can crush the caking fertilizer.

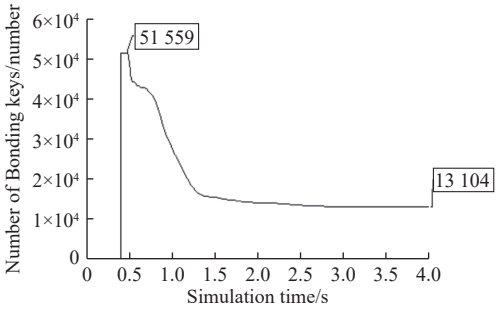

Figure 7 Variation of bonding bond number between particles

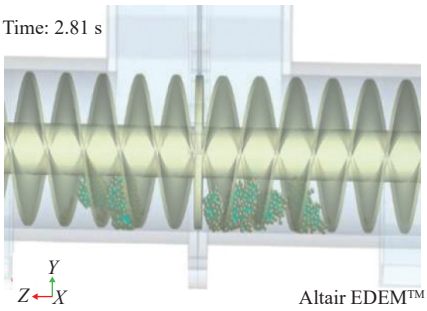

Figure 8 The particles fall into the fertilizer chamber and are discharged

3.3 Particle crushing test of agglomerated fertilizer

EDEM discrete element simulation results show that the crushing rate of the roller crushing device for a single agglomerated fertilizer particle reaches 74.6%, and the crushing effect is good. Now the actual crushing test is carried out on the agglomerated fertilizer particles to verify the crushing effect. The roller speed is set to the same 300 r/min. The fertilizer particles before crushing are shown in Figure 9a, and the fertilizer particles after crushing are shown in Figure 9b.

From Figure 9b, it is found that the broken fertilizer particles still have some caking, but the caking part can be discharged without blocking the fertilizer dispenser, which is consistent with the EDEM simulation results. EDEM discrete element simulation

and actual crushing test show that the roller crushing device has a good effect on the crushing of agglomerated fertilizer particles.

a. Caking fertilizer before crushing b. After crushing of agglomerated fertilizer

Figure 9 Caking fertilizer particle crushing test

4 Fertilizer discharge consistency simulation

In order to meet the requirements of soybean and corn strip composite planting, the two-way spiral fertilizer apparatus designed in this paper has two fertilizer outlets, which can fertilize two rows of soybean crops at the same time. The fertilization operation diagram is shown in Figure 10.

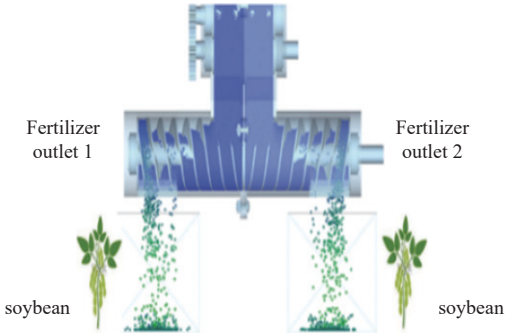

Figure 10 Two-way spiral fertilizer applicator fertilizer schematic diagram

4.1 EDEM simulation parameters

In order to verify whether the amount of fertilizer applied to the two rows of soybean crops is consistent when the two rows of fertilizer outlets are fertilized, the consistency of the fertilizer discharge device is simulated, and the EDEM related parameter settings are listed in Table 3.

Table 3 Diammonium phosphate particles EDEM parameter settings

Item	Attribute	Numerical value
Diammonium phosphate	Poisson ratio	0.25
	Elastic modulus/Pa	2.3×10^{7}
	Density/kg·m^{-3}	1635
Diammonium phosphate-diammonium phosphate	Coefficient of restitution	0.18
	Coefficient of static friction	0.26
	Coefficient of rolling friction	0.21
Diammonium phosphate-fertilizer shaft, shell	Coefficient of restitution	0.44
	Coefficient of static friction	0.53
	Coefficient of rolling friction	0.16

4.2 Simulation analysis

In the EDEM simulation test, the fertilizer application amount per acre was set to be 40 kg, the simulation operation width was set to be 0.75 m, and three operation gradients of 3 km/h, 4 km/h, and 5 km/h were set. The rotation speed of the fertilizer discharger was set to be 21.88, 29.18, and 36.48 r/min, respectively. The operation length is set to 2 m, and 20 collection chambers are set equidistantly. The difference of fertilizer application amount and the total fertilizer application amount of the two fertilizer outlets within the operation length of 2 m are measured to verify the consistent performance of the bidirectional spiral fertilizer discharge device. The process of simulation and data processing is shown in Figure 11.

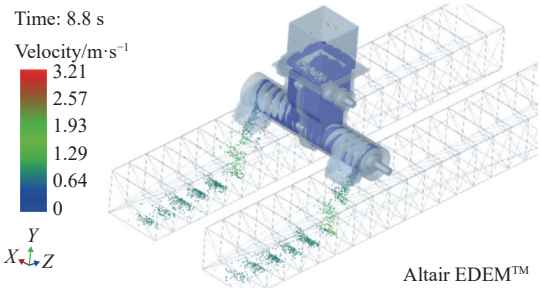

Figure 11 Test process and data processing

In EDEM, the speed of the fertilizer discharger, the particle factory, and other related settings are completed. The fertilizer particles in the particle factory are set to be dynamically generated, and the total mass generated is 1 kg. Using the post-processing function of EDEM software, the fertilizer information discharged from each fertilizer outlet was counted. At the end of the simulation, the data is imported into Origin software for data analysis.

4.3 Analysis of simulation results

After data processing by Origin data analysis software, the fertilizer amount information of the two-way spiral fertilizer distributor and the fertilizer discharge information of a single fertilizer outlet are obtained. The results are shown in Figure 12.

Through simulation, the total fertilization amount information of the fertilizer discharger at different operating speeds is obtained, as shown in Figure 12a. It was found that with the increase of operation speed, the total amount of fertilizer was gradually increased, which gradually exceeded the theoretical amount of fertilizer of 89.9 g. The analysis suggests that the increase in operating speed leads to a gradual rise in the rotational speed of fertilizer discharge. This acceleration causes the fertilizer particles to flow more quickly. When the simulation stops, a small amount of fertilizer particles continues to fall due to inertia, which results in an overall increase in fertilizer discharge. The information on the amount of fertilizer applied to each discharge port under the three operation gradients of 3 km/h, 4 km/h, and 5 km/h was counted and the statistical results are shown in Figure 13.

Taking the amount of fertilizer discharged from the fertilizer discharge port 1 as a benchmark, and comparing it with the fertilizer application information from the fertilizer discharge port 2, Table 4 is obtained. From the simulation data in the table, it can be seen that the fertilizer discharger's error in discharging the fertilizer from both fertilizer discharge ports is –1.6% at an operating speed of 3 km/h; the error in discharging the fertilizer from both fertilizer discharge ports is 3.3% at an operating speed of 4 km/h; and the error in discharging the fertilizer from both fertilizer discharge ports is 0.8% at an operating speed of 5 km/h. The error of fertilizer discharging from both rows was 0.8% at 5 km/h. The simulation results show that the fertilizer discharge device has good consistency and accuracy when fertilizing the two rows of crops, and meets the fertilization operation of the two rows of soybeans under the '4:2' mode of soybean-maize strip compound planting.

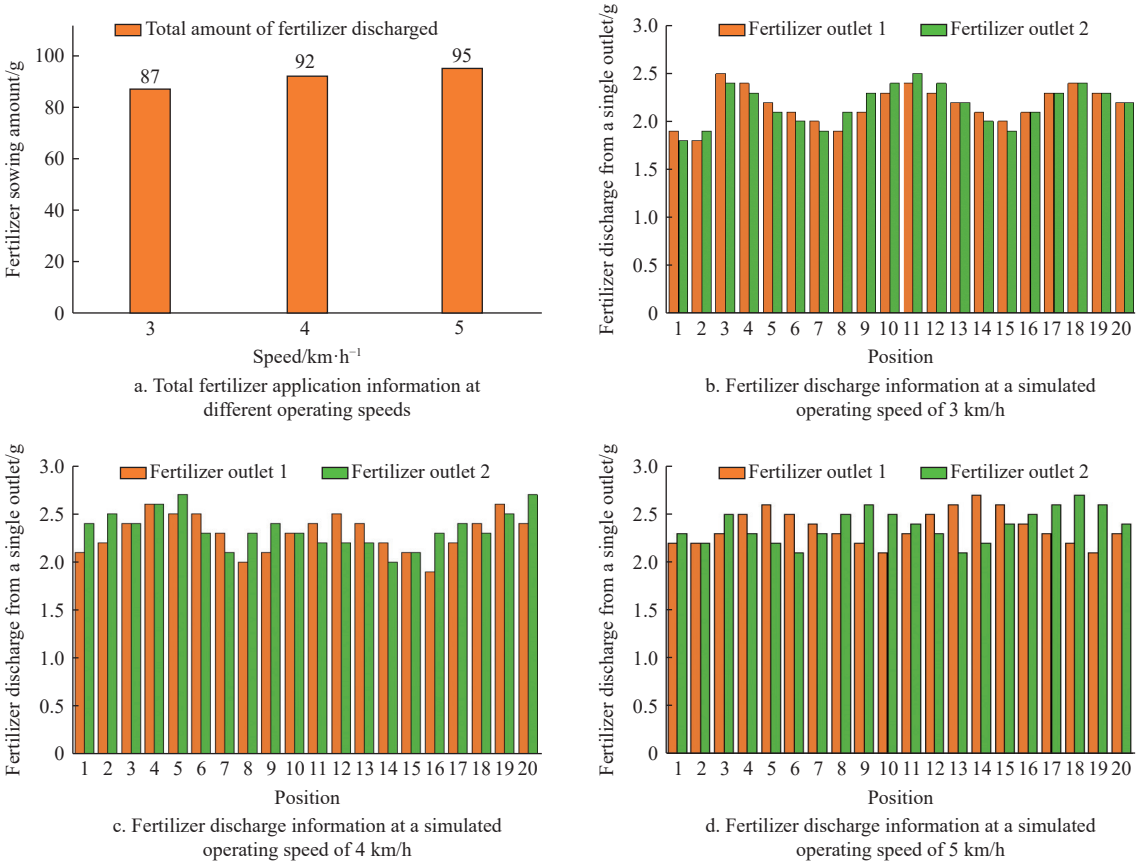

a. Total fertilizer application information at different operating speeds

b. Fertilizer discharge information at a simulated operating speed of 3 km/h

c. Fertilizer discharge information at a simulated operating speed of 4 km/h

d. Fertilizer discharge information at a simulated operating speed of 5 km/h

Figure 12 EDEM simulation results

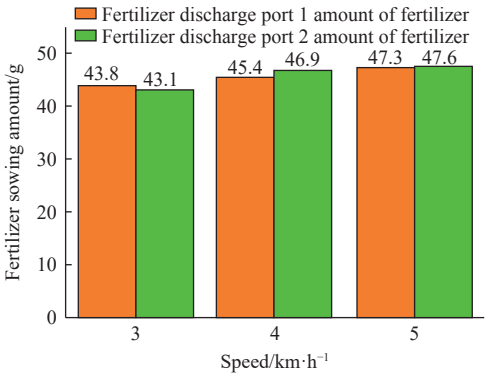

Figure 13 Comparison of the average amount of fertilizer discharged from the two rows of fertilizer outlets at different operating speeds

Table 4 Discharge Error Tab for Dual-Row Outlets of Bidirectional Spiral Fertilizer Distributor

Simulate operation speed/km·h⁻¹	Average amount of fertilizer discharged from fertilizer outlet 1/g	Average amount of fertilizer discharged from fertilizer outlet 2/g	Fertilization error/%
3	43.8	43.1	–1.6%
4	45.4	46.9	3.3%
5	47.3	47.7	0.8%

5 Split-drive variable fertilization control system design

Soybean and corn belt compound planting split-drive variable fertilization control system consists of two parts: first, the design of split-drive variable fertilization system, which is carried out according to the belt compound planting mode under the soybean belt, the corn belt, the 0.133 hm² of different fertilizer requirements, the use of PWM pulse signals to drive the soybean belt, the corn belt discharge motors, soybean belt, and corn belt, respectively, to achieve independent, variable control of the belt and the corn belt fertilizer; second, the design of 'GNSS + Encoder' dual speed measurement system, used to accurately obtain the operating speed of the implement. 'GNSS + encoder' dual speed measurement system is designed to accurately obtain the operating speed of the implements. With the roller crushing two-way spiral fertilizer discharger as the fertilization actuator, combined with the split-drive variable fertilization control system, the design of the split-drive variable fertilization system for soybean-maize strip compound planting was completed, and the variable fertilization operation under the soybean-maize strip compound planting mode was realized.

5.1 Design of split-drive variable fertilization system

The overall structure of soybean-maize split-drive variable fertilization system is shown in Figure 14. The system consists of multiple modules, including STM32 microcontroller, serial screen human-computer interaction module, GNSS positioning module, encoder speed measurement module, pre-filling fertilizer system, and soybean corn split-drive fertilization system.

The system obtains the information of fertilizer application rate of soybean and maize through human-computer interaction. The pre-filling fertilizer system reduces the lag distance of fertilization and improves the accuracy of fertilization by filling fertilizer in advance. After obtaining the operating speed of the fertilizer applicator through two speed measurement methods of GNSS and encoder, the data obtained by STM32 single-chip microcomputer comprehensive processing, combined with the current operating speed and the information of setting the amount of fertilizer per acre, the required speed of the soybean and corn fertilizer discharger

is calculated respectively, and the two-way PWM pulse signal is used to control the fertilization motor of the soybean belt and the corn belt respectively, so as to realize the separate-drive variable fertilization under the soybean-corn strip composite planting mode.

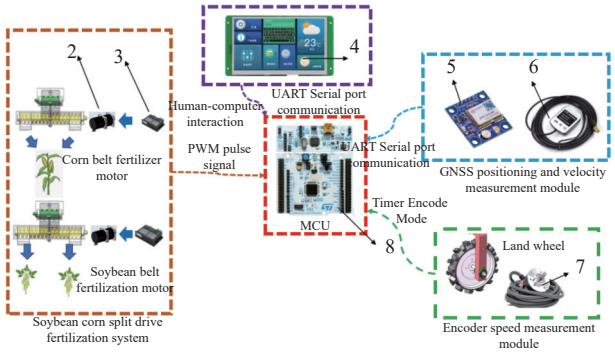

1. 24 V stepper motor 2. Stepper motor driver 3. 7-inch serial screen 4. GNSS positioning module 5.GNSS antenna 6.Omron coding 7.STM32F411RE microcontroller

Figure 14 Variable rate fertilization system composition

5.2 Split-drive variable fertilizer system

The split-drive variable-rate fertilization system is designed for the common '4:2' mode of soybean-maize strip compound planting in Huang-Huai-Hai region. The system includes two roller crushing two-way spiral fertilizer distributors. The roller crushing two-way spiral fertilizer discharger has two fertilizer outlets, and one fertilizer discharger can realize the fertilization operation of two rows of soybeans; through the docking of two fertilizer outlets, the fertilization operation of one row of corn after doubling the amount of fertilizer can meet the agronomic requirements of doubling the amount of fertilizer for corn, as shown in Figure 15. The fertilizer machine runs in the 'S' shape route to realize the fertilization operation of 4 rows of soybeans and 2 rows of corn, as shown in Figure 16.

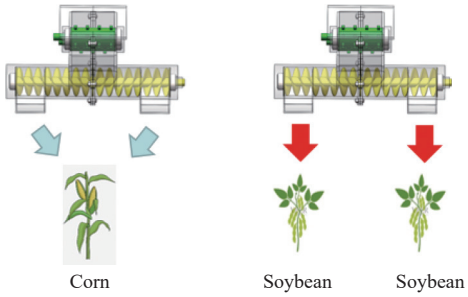

Figure 15 Two fertilizer dischargers realize the fertilization operation of soybean and corn

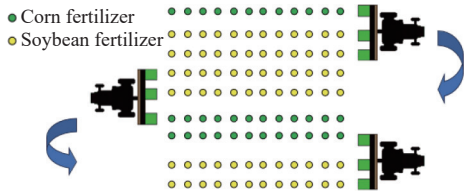

Figure 16 'S' route to realize the fertilization operation under the '4:2' mode

5.3 Split-drive variable fertilizer system workflow

The operation process of variable rate fertilization system is shown in Figure 17. The fertilizer application rate for soybean or corn is set through the serial port screen for human-computer interaction. After the start of the operation, the variable rate fertilization system first performs the pre-filling operation, and determines whether the pre-filling fertilizer is completed by the matrix optical fiber sensor installed at the fertilizer outlet. After the pre-filling fertilizer is completed, the STM32 single-chip microcomputer obtains the speed information of the fertilization operation through the 'GNSS + encoder' dual speed measurement system, and calculates the respective speeds of the soybean and corn fertilizer discharge motors in combination with the set fertilizer application rate of soybean or corn. The two PWM signals are sent to the stepper motor driver of the soybean belt and the corn belt respectively. The stepper motor driver then drives the stepper motor to rotate the soybean and corn fertilizer dischargers to adjust the speed of the two in real time to realize the variable fertilization operation.

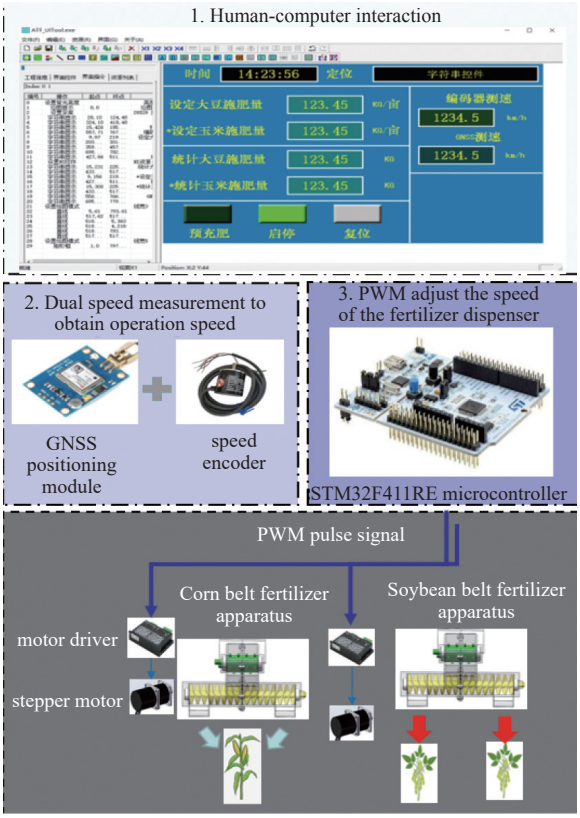

Figure 17 Variable fertilization operation process

In order to determine the optimal speed range of the encoder and the GNSS module, this paper uses the 2BYSF-3A fertilizer planter mounted on the tractor to simulate the fertilization operation at different speeds. By obtaining the respective speed values of the GNSS module and the encoder at different speeds and comparing which of the two is closer to the real speed and which has the smaller error, the optimal speed range of the two speed measurements is determined, which provides the basis for the subsequent speed measurement program to switch the speed source. The velocimetry test was conducted in the experimental field of Changyuan Branch of Henan Academy of Agricultural Sciences in Changyuan City, Henan Province, and the velocimetry equipment is shown in Figure 18.

Figure 18 Field test equipment

Due to the error between the display value of the tractor speed dashboard and the actual speed, it cannot be used as a reference standard in this test. To this end, this paper obtains the actual speed of the tractor operation through the following methods, that is, the test sets a 20 m-long path, lets the tractor enter the field at a constant speed outside the 20 m field, and runs 20 m, and calculates the tractor operation speed by calculating the time required to run 20 m. Different operating speeds are obtained by setting the same gear and different throttle sizes by the tractor. Through the experiment, the speed values measured by the encoder and the GNSS module are obtained under the conditions of 1.8, 3.7, 5.5, and 7.4 km/h of the tractor, respectively, as shown in Figure 19.

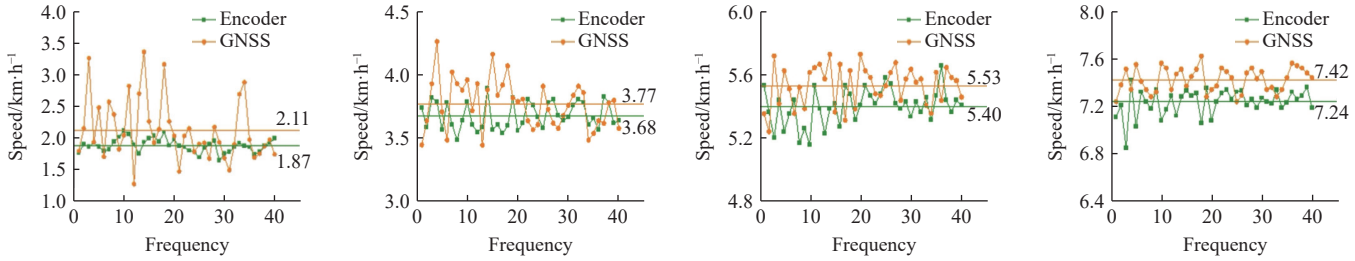

a. 1.8 km/h b. 3.7 km/h c. 5.5 km/h d. 7.4 km/h

Figure 19 Speed values measured by the encoder and GNSS change under different operating speed conditions

The experimental data is calculated in Table 5, which shows the minimum, maximum, median, mean, and coefficient of variation of the data measured by encoder 1 and GNSS module 3 at different speeds.

Table 5 Field test data related results

Speed/ km·h⁻¹	Item	Min value/ km·h⁻¹	Max value/ km·h⁻¹	Average/ km·h⁻¹	Standard deviation	Coefficient of variation/%
1.8	Encoder	1.63	2.1	1.87	0.105 77	5.661
	GNSS module	1.26	3.35	2.11	0.4899	23.251
3.7	Encoder	3.49	3.65	3.68	0.104 41	2.836
	GNSS module	3.45	4.26	3.77	0.1915	5.079
5.5	Encoder	5.17	5.65	5.40	0.108 01	1.999
	GNSS module	5.25	5.72	5.53	0.123 13	2.196
7.4	Encoder	6.85	7.42	7.24	0.110 34	1.525
	GNSS module	7.24	7.62	7.42	0.100 69	1.357

According to the data, when the tractor travels at a speed of 1.8 km/h, the speed value measured by the encoder through the ground wheel is relatively stable, with an average of 1.87 km/h and a coefficient of variation of 5.661%. The average value measured by GNSS is 2.11 km/h, and the coefficient of variation is 23.251%. At 3.7 km/h, the average speed measured by the encoder is 3.68 km/h, and the coefficient of variation is 2.836%. The average value obtained by GNSS is 3.77 km/h, and the coefficient of variation is 5.079%. At 5.5 km/h, the average speed measured by the encoder is 5.4 km/h, and the coefficient of variation is 1.999%. The average speed of GNSS is 5.53 km/h, and the coefficient of variation is 2.196%. At 7.4 km/h, the average speed measured by the encoder is 7.24 km/h, the coefficient of variation is 1.525%, the average speed of GNSS is 7.42 km/h, and the coefficient of variation is 1.357%. The operating speed is set as the *X*-axis, and the difference between the speed measurement value of the encoder and the GNSS module and the actual operating speed is set as the *Y*-axis. According to the test data, the line chart of the speed measurement error under different speed conditions is obtained, as shown in Figures 20a and 20b. The velocity measurement error of the two is placed in the same diagram, and the comparison line diagram of the velocity measurement error of the two is obtained.

It can be seen from Figure 20c that as the working speed increases, the encoder speed measurement error decreases first and then increases. The velocity measurement error of the GNSS module gradually decreases with the increase of the operating speed. The Origin data analysis software is used to non-linearly fit the changing trend of the two, and the fitting curve of the velocity error of the two is obtained, as shown in Figure 21.

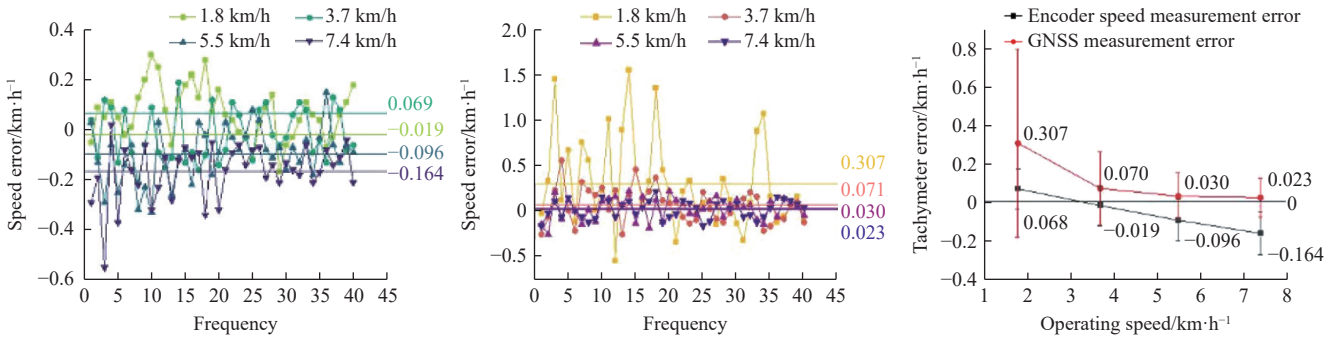

a. Encoder speed error change b. GNSS Velocimetry Error Variation c. Comparison of velocity error between the two

Figure 20 Change of velocity error between encoder and GNSS at different speeds

Referring to the relevant literature[14,27], and considering the relevant research results of various scholars and the results of field experiments, the dual speed measurement system designed in this paper selects the encoder speed value when the encoder speed value is less than or equal to 4.5 km/h. When the working speed measured by the encoder is higher than 4.5 km/h, the GNSS module is used to measure the speed. The relevant code is written in the Keil μVision v5 development tool, and the judgment value of the speed switching interval is set to 4.5 km/h. The workflow of the speed measurement system is shown in Figure 22.

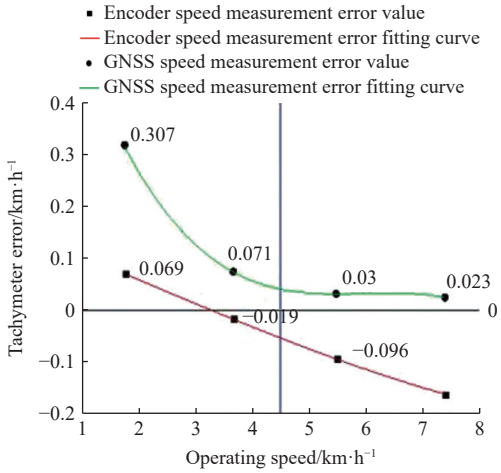

Figure 21 Tachymeter error trend chart

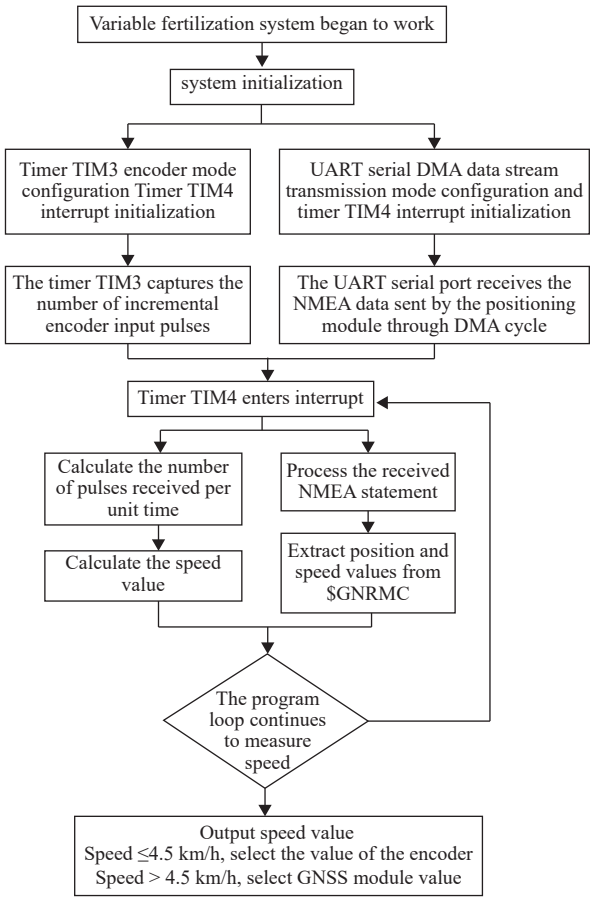

Figure 22 Flow chart of the system measuring speed

6 Fertilizer discharge calibration

6.1 Fertilizer discharge calibration test

The theoretical fertilizer discharge equation, and the actual fertilizer application operation of soybean belt and corn belt fertilizer discharge motor speed must be different. Therefore, it is necessary to calibrate the actual fertilizer discharge amount of the two-way spiral fertilizer discharger under different rotational speeds through the bench test, and obtain the actual corresponding relationship between the rotational speed of the fertilizer discharger, the working speed and the fertilizer application amount per acre when the fertilizer discharger is applied with urea and diammonium phosphate, so as to guide the field variable fertilization operation.

6.2 Test equipment

In order to make the amount of fertilizer in the test closer to the actual operation, the calibration test of the amount of fertilizer was carried out on the modified Henan Nongyouwang 2BYSF-3A fertilizer planter, as shown in Figure 23. At the same time, the information of the amount of fertilizer discharged by each fertilizer outlet when the fertilizer discharger is applied with diammonium phosphate is counted, and the consistency of the fertilizer discharger is verified, as shown in Figure 23b.

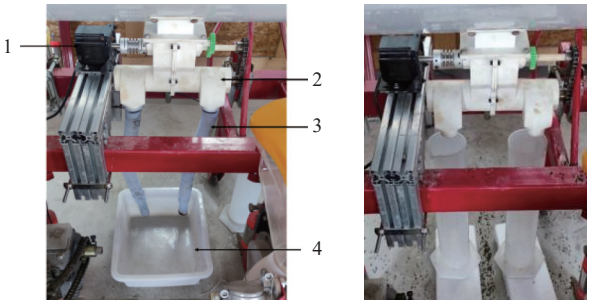

a. Urea fertilizer measurement b. Diammonium phosphate fertilizer measurement

1. Stepping motor 2. Roller crushing two-way spiral fertilizer discharger 3. Fertilizer discharge tube 4.Tray

Figure 23 Fertilizer discharge calibration bench

The ACS-JS-10 electronic scale is used to weigh the chemical fertilizer with an accuracy of ±0.1 g. The parameters are shown in Table 6.

Table 6 ACS-JS-10 Electronic scale parameters

Item	Parameter
Weighing range/kg	0-10
Precision/g	±0.1
Scale plate size/mm	280×200
Power supply	220 V AC or 6 V battery

6.3 Fertilizer discharge calibration test and result analysis

In the experiment, three gradients were set for the rotation speed of the fertilizer discharger, and one gradient was set every 30 r/min in the range of 10-80 r/min. The amount of fertilizer discharged when urea and diammonium phosphate were applied within 1 minute under each gradient was measured, and the amount of fertilizer applied per acre corresponding to the two velocity gradients in the range of 1-7 km/h was calculated. Tables 7 and 8 show the information on the amount of fertilizer discharged obtained by applying urea and diammonium phosphate at different rotational speeds and operating speeds of the fertilizer discharger and the information on the amount of fertilizer applied to the corresponding hm^2, respectively.

In the statistics of the amount of fertilizer discharged when the diammonium phosphate is applied to the fertilizer discharger, the information of the amount of fertilizer discharged per minute at each fertilizer outlet is collected. Based on the amount of fertilizer

discharged from the fertilizer outlet 1, the difference in the amount of fertilizer discharged from the two fertilizer outlets is obtained (Table 9). Table 9 shows that the maximum error of the amount of fertilizer discharged by the two rows of fertilizer outlets of the two-way spiral fertilizer dispenser at different speeds is 2.88%, and the minimum is 0%, which is close to the simulation results. It is proved that the two rows of fertilizer outlets of the fertilizer dispenser have good consistent performance.

Table 7 Corresponding urea fertilizer discharge under different rotational speeds and operating speeds

Revolution speed/r·min^{-1}	Fertilizer sowing amount/kg·min^{-1}	Fertilizer application rate under different operating speed/kg·hm^{-2}						
		1 km·h^{-1}	2 km·h^{-1}	3 km·h^{-1}	4 km·h^{-1}	5 km·h^{-1}	6 km·h^{-1}	7 km·h^{-1}
10	0.601	290.820	145.410	96.945	72.705	58.170	48.465	41.550
20	1.110	537.120	268.560	179.040	134.280	107.430	89.520	76.725
30	1.584	766.485	383.250	255.495	191.625	153.300	127.755	109.500
40	2.112	1021.980	510.990	340.665	255.495	204.390	170.325	145.995
50	2.478	1199.085	599.550	399.690	299.775	239.820	199.845	171.300
60	2.940	1422.645	711.330	474.210	355.665	284.535	237.105	203.235
70	3.420	1654.920	827.460	551.640	413.730	330.990	275.820	236.415
80	4.062	1965.585	982.785	655.200	491.400	393.120	327.600	280.800

Table 8 Fertilizer discharge of diammonium phosphate corresponding to different rotational speeds and operating speeds

Revolution speed/r·min^{-1}	Fertilizer sowing amount/kg·min^{-1}			Fertilizer application rate under different operating speed/kg·hm^{-2}						
	Fertilizer outlet 1	Fertilizer outlet 2	Average	1 km·h^{-1}	2 km·h^{-1}	3 km·h^{-1}	4 km·h^{-1}	5 km·h^{-1}	6 km·h^{-1}	7 km·h^{-1}
10	0.312	0.321	4.755	303.855	151.935	101.28	75.960	60.765	50.640	43.410
20	0.654	0.645	0.650	623.550	311.775	207.855	155.895	124.710	103.920	89.085
30	0.955	0.964	0.960	921.165	460.590	307.050	230.295	184.230	153.525	131.595
40	1.237	1.230	1.234	134.220	592.110	394.740	296.055	236.850	197.370	169.170
50	1.542	1.545	1.544	1481.835	740.910	493.950	370.455	296.370	246.975	211.695
60	1.782	1.782	1.782	1710.810	855.405	570.270	427.695	342.165	285.135	244.395
70	2.206	2.207	2.207	2118.345	1059.180	706.110	529.590	423.675	353.055	302.625
80	2.656	2.656	2.661	2554.215	1277.100	851.400	638.550	510.840	425.700	364.890

Table 9 Error tab of two rows of fertilizer outlets of two-way spiral fertilizer distributor

Revolution speed/r·min^{-1}	Fertilizer sowing amount/kg		Error/%
	Fertilizer outlet 1	Fertilizer outlet 2	
10	0.312	0.321	2.88%
20	0.654	0.645	–1.38%
30	0.955	0.964	0.94%
40	1.237	1.230	–0.57%
50	1.542	1.545	0.19%
60	1.782	1.782	0.00%
70	2.206	2.207	0.05%
80	2.656	2.665	0.34%

7 Field trial

The field experiment site was the experimental field of Changyuan Branch of Henan Academy of Agricultural Sciences, Changyuan City, Henan Province (35.428°N, 114.289°E). The test materials include: 100 m tape, urea 50 kg, diammonium phosphate 40 kg, ACS-JS-10 electronic scale, modified Henan Nongyouwang soybean corn strip compound planting '4:2' mode 2BYSF-3A fertilization seeder, John Deere 604 tractor, plastic bag (Figure 24).

Figure 24 Field test equipment

7.1 Field experiment scheme

The evaluation of fertilization accuracy in field trials was calculated according to Equation (21) in the 'Fertilizer Precision Control Method' in the 'GB/T 35487-2017 Variable Fertilizer Planter Control System':

$$\delta_2 = \frac{(G_1 - G_2)}{G_2} \times 100\% \tag{21}$$

where, δ_2 is variable fertilization control precision; G_1 is actual fertilizer discharging mass, kg; G_2 is theoretical fertilizer discharging mass, kg.

The theoretical fertilizer under feed mass G_2 was calculated according to Equation (22):

$$G_2 = L_2 \times A_2 / 10\,000 \tag{22}$$

where, L_2 is preset discharging volume of fertilizer application, kg/hm^2; A_2 is operating area, hm^2.

Field experiment method of variable rate fertilization system: three gradients of 150 kg/hm^2, 225 kg/hm^2, and 300 kg/hm^2 were set for soybean belt fertilization. The amount of fertilizer applied to the corn belt was set at three gradients of 600 kg/hm^2, 750 kg/hm^2, and 900 kg/hm^2.

The tractor-mounted composite planter for soybean and corn operates at three different speeds: 3 km/h, 4 km/h, and 5 km/h. This planter is used for fertilization in both soybean and corn belts, across three different fertilizer gradients, as illustrated in Figure 25a. The width of the seeder is 1.25 m, with a working length of 10 m, resulting in 12.5 m^2. Two plastic bags are used to collect the soybean fertilizer for each fertilizer outlet, as shown in Figure 25b. Corn fertilizer was collected using a plastic bag, as shown in Figure 25c.

a. Field test diagram b. Soybean fertilizer collection c. Corn fertilizer collection

Figure 25 Field experiment and fertilizer collection

7.2 Test results and analysis

The results of the field trials are shown in Tables 10 and 11.

Table 10 Soybean variable rate fertilization results

Set the amount of fertilizer/ kg·hm^{-2}	Operating speed/ km·h^{-1}	Theoretical fertilization amount/kg	Actual fertilizer application/kg			Error/ %
			Fertilizer outlet 1	Fertilizer outlet 2	Total fertilization	
150	3	0.187	0.095	0.087	0.182	–2.67
	4		0.098	0.091	0.189	1.07
	5		0.101	0.095	0.196	4.81
225	3	0.281	0.141	0.136	0.277	–1.42
	4		0.149	0.142	0.291	3.56
	5		0.144	0.145	0.289	2.85
300	3	0.375	0.185	0.181	0.366	–2.40
	4		0.196	0.188	0.384	2.40
	5		0.188	0.198	0.386	2.93

Table 11 Results of corn variable fertilization operation

Set the amount of fertilizer/ kg·hm^{-2}	Operating speed/km·h^{-1}	Theoretical fertilization amount/kg	Actual fertilizer application/kg	Error/ %
600	3	0.750	0.739	–1.47
	4		0.785	4.67
	5		0.776	3.47
750	3	0.937	0.921	–1.71
	4		0.955	1.92
	5		0.961	2.56
900	3	1.125	1.139	1.24
	4		1.118	–0.62
	5		1.131	0.53

From the field test results:

(1) The best accuracy of 4.81% for the soybean belt fertilization occured at the fertilization amount of 150 kg/hm^2 and the operation speed of 5 km/h, which meets the standard of variable fertilization of 5% required in the ‘GB/T 35487-2017 variable fertilization seeder control system.

8 Conclusions

(1) Aiming at the problem of caking fertilizer congestion and poor uniformity of fertilizer discharge, a two-way spiral fertilizer discharge device for roller crushing was designed. The crushing process and fertilizer discharge consistency of caking fertilizer particles were simulated by theoretical calculation and EDEM. The simulation results of particle crushing showed that the crushing rate of caking fertilizer particles by the roller crushing device reached 74.6%. The simulation results of the consistency of fertilizer discharge show that when the simulation operation speed is at 3, 4, and 5 km/h, the fertilizer discharge errors of the two rows of fertilizer outlets of the fertilizer discharger are -1.6%, 3.3%, and 0.8%, respectively, and the consistency of fertilizer discharge is good.

(2) The split-drive variable-rate fertilization system was designed. The roller crushing two-way spiral fertilizer discharger was used as the core component. The structure design of the soybean-maize strip compound planting split-drive fertilization system, the selection and control of the fertilizer discharge motor, the UART communication between the STM32 microcontroller and the serial port screen, the structure design of the power system, the application of the GNSS positioning and speed measurement module, and the application of the encoder speed measurement module realized the separate control of the fertilizer amount of the soybean belt and the corn belt.

(3) Aiming at the problems of low speed accuracy of encoder at high speed and low speed accuracy of GNSS module at low speed, a ‘GNSS + encoder’ double speed measurement system is designed. It includes GNSS module and encoder module selection application, NMEA information interception, single-chip microcomputer speed measurement program design, and field speed measurement test. The field speed test results show that when the working speed of the machine is less than 4.5 km/h, the encoder speed measurement error is less than GNSS; when the working speed of the machine is greater than 4.5 km/h, the encoder speed measurement error is greater than GNSS. The dual speed measurement system takes 4.5 km/h as the node to realize the switching of the speed measurement source of the variable fertilization system between the encoder and the GNSS module.

(4) Bench and field experiments were carried out for the separate-drive variable rate fertilization system. Through the bench test, the fertilizer discharge amount of the fertilizer discharger was calibrated, and the mathematical relationship models of ‘fertilizer application amount per acre-operating speed-fertilizer discharger speed’ of soybean belt and corn belt were established, and the consistency of fertilizer discharger was verified. The results showed that the error of fertilizer discharge amount of the two fertilizer outlets of the fertilizer discharger at different speeds was less than or equal to 2.88%. The results of field experiment showed that the maximum error of soybean belt was 4.81% when the fertilization amount was 150 kg/hm^2 and the operation speed was 5 km/h. The maximum error was 4.67% when the fertilizer application rate was 600 kg/hm^2 and the operation speed was 4 km/h. The maximum error of both is less than 5%, which meets the requirements of variable fertilization.

Acknowledgements

This research was supported by China Agriculture Research System of MOF and MARA (CARS-04), National Key Research and Development Program of China (Grant No. 2022YFD2300904), and the Key Scientific and Technological Project of Henan Province Department of China (Grant No. 252102111171).

[References]

[1] Xu C B, Dong W J, Li H P, Yu Q L, Zhang C H, Ding Y C. Design and experiment of a centrifugal cavity disc extrusion type high-speed precision fertilizer apparatus for rapeseed. Transactions of the CSAE, 2024; 40(20): 22–34.

[2] Xiao W L, Liao Y T, Shan Y Y, Li M L, Wang L, Liao Q X. Design and experiment of quad-screw double-row fertilizer apparatus for rape seeding machine. Transactions of the CSAM, 2021; 52(11): 68–77.

[3] Wang J F, Fu Z D, Weng W X, Wang Z T, Wang J W, Yang D Z. Design and experiment of conical-disc push plate double-row fertilizer apparatus

for side-deep fertilization in paddy field. Transactions of the CSAM, 2023; 54(2): 53–62. doi:10.6041/j.issn.1000-1298.2023.02.005

[4] Qi J T, Tian X L, Li Y, Fan X H, Yuan H F, Zhao J L, et al. Design and experiment of a subsoiling variable rate fertilization machine. Int J Agric & Biol Eng, 2020; 13(4): 118–124.

[5] Bangura K, Wu S L, Tang Z Y, Feng X, Hu R J, Cai Y H, et al. Design and performance evaluation of the six-row side deep fertilizer applicator for paddy fields. Int J Agric & Biol Eng, 2024; 17(6): 166–175.

[6] Campbell C M, Fulton J P, Mcdonald T P, Wood C W, Zech W C, Srivastava P. Spinner-disc technology to enhance the application of poultry litter. Applied Engineering in Agriculture, 2010; 26(5): 759–767.

[7] Michálek T, Zelenka J. Modelling of flexi-coil springs with rubber-metal pads in a locomotive running gear. Applied & Computational Mechanics, 2015; 9(1): 21–30.

[8] Shi Y Y, Hu Z Z, Wang X C, Odhiambo M O, Sun G X. Fertilization strategy and application model using a centrifugal variable-rate fertilizer spreader. Int J Agric & Biol Eng, 2018; 11(6): 41–48.

[9] Chang Y K, Zaman Q U, Farooque A, Chattha H, Schumann A. Sensing and control system for spot application of granular fertilizer in wild blueberry field. Precision Agriculture, 2016; 18(2): 210–223.

[10] Zhu H X, Tan H. Research on the performance of spiral conveyer based on EDEM. Mechanical & Electrical Engineering Technology, 2018; 47(7): 27–29. doi:10.3969/j.issn.1009-9492.2018.07.009

[11] Transport machinery design selection manual. Chemical Industry Press, 2004.

[12] Chen X F, Luo X W, Wang Z M, Zhang M H, Hu L, Yang W W, et al. Design and experiment of a fertilizer distribution apparatus with double-level screws. Transactions of the CSAE, 2015; 31(3): 10–16. doi: 10.3969/j.issn.1002-6819.2015.03.002

[13] Han C J, Liu Z, Mao H P, Ma X, Wang S. Design and experiment of variable rate fertilization combined soil preparation machine. Transactions of the CSAM, 2024; 55(11): 250–261. doi:10.3969/j.issn.1009-9492.2018.07.009

[14] Zhao X G, Jin X, Zou W, Zhai C Y, Zhang C F, Wang X. Design and experiment of double speed measurement mode of corn topdressing control system based on spectral information. Transactions of the CSAM, 2020; 51(S1): 145–153. doi:10.6041/j.issn.1000-1298.2020.S1.017

[15] Chen G B, Wang Q J, Li W Y, He J, Li H W, Yu C C. Design and experiment of double roller differential speed crushing fertilizer device for block organic fertilizer. Transactions of the CSAM, 2021; 52(12): 65–76.

[16] Sun K K, Ma R D, Li G. The influence of the structure of double toothed roller crusher on the crushing effect based on EDEM. 4th International Conference on Applied Materials and Manufacturing Technology: ICAMMT 2018, Nanchang, China, 25-27 May 2018.

[17] Ma X, Zhao X, Liu S S, Wang Y W, Wang X C, Li Z H. Design and experiment of solid particle fertilizer variable rate fertilization device for high-speed rice transplanter. Transactions of the CSAM, 2023; 54(9): 99–110.

[18] Wang J F, Lü Z Y, Zhao M Y, Wang Z T. Design and experiment of rice side-deep variable rate fertilization control system based on prescription diagrams. Transactions of the CSAM, 2024; 55(9): 151–162.

[19] Cao X P, Wang Q J, Li H W, He J, Lu C Y. Combined row cleaners research with side cutter and stubble clean disk of corn no-till seeder. Transactions of the CSAM, 2021; 52(3): 36–44.

[20] Liu G, Hu H, Huang J Y, Zhang J Q. Lag time detection and position correction method of variable rate fertilization. Transactions of the CSAM, 2021; 52(S1): 74–80.

[21] Zhang J Q, Liu G, Hu H, Huang J Y, Liu Y J. Influence of control sequence of spiral fluted roller fertilizer distributer on fertilization performance. Transactions of the CSAM, 2020; 51(S1): 137–144.

[22] Zhang J Q, Liu G, Hu H, Huang J Y. Development of bivariate fertilizer control system via independent control of fertilizing unit. Transactions of the CSAE, 2021; 37(10): 38–45.

[23] Kim K C, Jiang T, Kwon C L, Kwon C. Effects of ball-to-powder diameter ratio and powder particle shape on EDEM simulation in a planetary ball mill. Journal of the Indian Chemical Society, 2022; 99(1): 100300.

[24] Li C, Li Z, Wang T, Ling G X, Wang S F, Li J. Parameter optimization of column-comb harvesting of litchi based on the EDEM. Scientia Horticulturae, 2023; 321: 112216.

[25] Zhang P C, Li F G, Wang F Y. Optimization and test of ginger shaking and harvesting device based on EDEM software. Computers and Electronics in Agriculture, 2023; 213: 108257.

[26] Wen X Y, Jia H L, Zhang S W, Yuan H F, Wang G, Chen T Y. Test of suspension velocity of granular fertilizer based on EDEM-Fluent coupling. Transactions of the CSAM, 2020; 51(3): 69–77. doi:10.6041/j.issn.1000-1298.2020.03.008

[27] Karayel D. Performance of a modified precision vacuum seeder for no-till sowing of maize and soybean. Soil Tillage Research, 2009; 104(1): 121–125.